

Receptor tyrosine kinase expression and phosphorylation in canine nasal carcinoma

By

Samuel Hocker

B.S., Illinois State University, 2008  
D.V.M., Kansas State University, 2012

A THESIS

submitted in partial fulfillment of the requirements for the degree

MASTER OF SCIENCE

Department of Clinical Sciences  
College of Veterinary Medicine

KANSAS STATE UNIVERSITY  
Manhattan, Kansas

2018

Approved by:

Major Professor  
Mary Lynn Higginbotham

# **Copyright**

© Samuel Hocker 2018.

## Abstract

This study evaluated sixteen canine nasal carcinoma and five normal nasal epithelium samples for expression and phosphorylation of known targets of toceranib [vascular endothelial growth factor receptor-2 (VEGFR2), platelet derived growth factor alpha (PDGFR- $\alpha$ ), platelet derived growth factor receptor beta (PDGFR- $\beta$ ), and stem cell factor receptor (c-KIT)] and epidermal growth factor receptor 1 (EGFR1) using immunohistochemistry, RT-PCR and a receptor tyrosine kinase (RTK) phosphorylation panel. Protein for VEGFR2 was expressed in neoplastic cells of all carcinomas, PDGFR- $\alpha$  was noted in 15/16, whereas PDGFR- $\beta$  was detected in 3/16 samples, but showed primarily stromal staining. Protein expression for c-KIT was present in 4/16 and EGFR1 was noted in 14/16 samples. Normal tissue showed variable protein expression of the RTKs. Messenger RNA for VEGFR2, PDGFR- $\beta$ , and c-KIT were noted in all samples. Messenger RNA for PDGFR- $\alpha$  and EGFR1 were detected in 15/16 samples. All normal nasal tissue detected messenger RNA for all RTKs of interest. Constitutive phosphorylation of VEGFR2, PDGFR- $\alpha$ , PDGFR- $\beta$  and c-KIT was not observed in any carcinoma or normal nasal sample, but phosphorylation of EGFR1 was noted in 10/16 carcinoma and 3/5 normal samples. The absence of major phosphorylated RTK targets of toceranib suggests the clinical effect of toceranib may occur through inhibition of alternative and currently unidentified RTK pathways in canine nasal carcinomas. The observed protein and message expression and phosphorylation of EGFR1 in the nasal carcinoma samples merits further inquiry into EGFR1 as a therapeutic target for this cancer.

## Table of Contents

List of Figures.....	v
List of Tables.....	vi
Acknowledgements.....	vii
Chapter 1 – Introduction.....	1
Chapter 2 – Approach to Research.....	4
Immunohistochemistry.....	4
RNA isolation and RT-PCR.....	5
Cell lysate preparation and phosphoprotein arrays.....	6
Chapter 3 – Results.....	9
Chapter 4 – Discussion.....	14
Chapter 5 – Conclusions.....	17
References.....	18
Appendix A – Abbreviations.....	23
Appendix B - Complete Phospho-RTK Results.....	25

## **List of Figures**

Figure 3.1 Immunohistochemistry for VEGFR2, PDGFR $\alpha/\beta$ , KIT, & EGFR.....	11
Figure 3.2 Phospho-RTK arrays of canine nasal carcinomas.....	13

## **List of Tables**

Table 2.1 Primer sequences used in RT-PCR.....	8
Table 3.1 Nasal carcinoma RTK expression by IHC.....	10
Table 3.2 Nasal carcinoma qualitative messenger RNA expression by RT-PCR.....	12
Table 3.3 Nasal carcinoma phosphoprotein results.....	12

## **Acknowledgements**

Thank you to Allison Goldberg for her assistance in RT-PCR preparation; Dr. Annelise Nguyen and Leigh Feuerbacher for their assistance in molecular techniques and analysis.

This study was funded by the Mark Derrick Canine Research Fund and the Kansas State University, College of Veterinary Medicine MCAT grant.

Thank you to Jennifer Phinney and the KSVDL histology and immunohistochemistry laboratory for development of IHC assays, staining and digitizing of slides for analysis.

## Chapter 1- Introduction

Epithelial tumors, including adenocarcinoma, squamous cell carcinoma, and undifferentiated carcinoma, comprise nearly two-thirds of canine intra-nasal neoplasia.<sup>1,2</sup> These tumors are characterized by progressive local invasion and a low metastatic rate at the time of initial diagnosis, but may be as high as 40-50% at the time of death.<sup>3</sup> The cause of death in most patients is typically attributable to extensive primary disease rather than the presence of metastasis. Owing to this biologic behavior, external beam radiation therapy is the treatment of choice for canine intranasal tumors. Radiation therapy substantially improves survival, with median survival times of 7-23 months compared to 3 months for those patients that do not receive any form of treatment.<sup>4-7</sup> Despite most dogs experiencing a favorable response to treatment, the majority of dogs treated with radiation therapy will experience tumor recurrence and suffer from progressive disease. In lieu of radiation therapy or when tumor recurrence is documented after radiation therapy, some owners may elect to pursue other treatment options such as chemotherapy.

Protein kinases are normal regulators of cell signaling that act through phosphorylation of other proteins and are stimulated by growth factors. Protein kinases can be expressed on the cell surface, cytoplasm, or even the nucleus. Toceranib phosphate (Palladia®, Pfizer Animal Health, Madison, NJ, USA) is an FDA-approved canine drug that is a multi-kinase inhibitor that was developed to inhibit stem cell factor (c-KIT), a receptor tyrosine kinase (RTK) that is mutated in approximately 30% of canine mast cell tumors.<sup>8</sup> Multi-kinase inhibitors like toceranib work by blocking the ability of the kinase to bind ATP, as this is necessary for donating the phosphate group that phosphorylates the tyrosine kinase as well as downstream targets. The first clinical evaluation of toceranib in veterinary medicine was a phase I clinical trial evaluating safety and



activity of the drug in dogs with a variety of tumor types. Mast cell tumors exhibited the highest frequency of response, but evidence for anti-tumor activity of toceranib was found in 54% of other treated cases including patients with carcinomas, sarcomas, melanoma, and multiple myeloma.<sup>9</sup> More recently, efficacy of toceranib phosphate has been retrospectively evaluated in a variety of solid tumor types, including nasal carcinomas.<sup>10</sup> Dogs receiving toceranib in this study exhibited a resolution of clinical signs, with one dog having an objectively measured complete response and another with stable disease, indicating toceranib phosphate may possess a role in the treatment of canine nasal carcinomas. Toceranib phosphate inhibits the activity of several RTKs linked to cancer biology including: vascular endothelial growth factor receptor 2 (VEGFR2), platelet derived growth factor receptor  $\alpha$  (PDGFR- $\alpha$ ), platelet derived growth factor receptor  $\beta$  (PDGFR- $\beta$ ), FMS-like tyrosine kinase 3 (FLT-3), colony stimulating factor receptor 1 (CSFR1), and stem cell factor receptor (c-KIT).<sup>11</sup> With this spectrum of inhibition, toceranib can act as an oral anti-angiogenic agent in those tumors that exhibit angiogenic RTKs such as VEGFR2, PDGFR- $\alpha$ , and PDGFR- $\beta$ .<sup>9,12</sup>

Several RTK targets of toceranib expressed by canine nasal carcinomas are responsible for angiogenic sprouting and vascular maturation, both defined processes in vasculogenesis and angiogenesis that are imperative for tumor growth.<sup>9,12-14</sup> In one report of 187 dogs with nasal carcinoma, VEGFR was detected in 84.5%, PDGFR- $\alpha$  in 71.1%, and PDGFR- $\beta$  in 39.6% of tumors by immunohistochemistry.<sup>13</sup> While VEGFR was expressed in the majority of these canine nasal carcinomas, another report showed that 91.7% of epithelial nasal tumors also expressed the VEGF ligand.<sup>14</sup> Additionally, one report of dogs with solid tumors treated with toceranib identified significantly increased plasma VEGF level, a surrogate marker for VEGFR2 inhibition, denoting a possible anti-angiogenic effect.<sup>15</sup> Although potential RTK targets are

present in canine nasal carcinomas, it is not known whether their constitutive phosphorylation is a direct underlying mechanism of toceranib's activity.

Epidermal growth factor receptor expression has been noted in a variety of canine tumors including transitional cell carcinoma, mammary carcinomas, gliomas, and pulmonary adenocarcinoma.<sup>16-19</sup> Canine nasal carcinomas have also been shown to express epidermal growth factor receptor 1 (EGFR1) in 55% of tumors.<sup>14</sup> Epidermal growth factor receptor is the principal RTK expressed in human head and neck tumors and represents a therapeutic target for humans afflicted with this type of cancer.<sup>20,21</sup> Based on kinome analysis, EGFR1 activity is not inhibited by toceranib, but it may represent a future therapeutic target for dogs with nasal carcinoma.<sup>22</sup>

In light of toceranib's spectrum of RTK inhibition and clinical activity against canine nasal carcinomas, the intent of this study was to assess this tumor type for the phosphorylation of VEGFR2, PDGFR $\alpha$ , PDGFR- $\beta$ , and c-KIT and to subsequently verify the protein and messenger RNA expression of these RTKs to obtain a more detailed understanding into their functional relationship with toceranib's efficacy. A secondary aim of this study was to evaluate the phosphorylation of EGFR1, as well as a panel of other RTKs, and to demonstrate expression of EGFR1 at the messenger RNA and protein level to validate EGFR1 as a prospective target in the treatment of canine nasal carcinomas. With these objectives, it was hypothesized that canine nasal carcinoma expresses a complement of RTKs involved in tumor growth and metastasis and are targets of toceranib phosphate. Additionally, it was hypothesized that targets of toceranib are constitutively phosphorylated in canine nasal carcinoma.

## Chapter 2 – Approach to Research

Nasal tissue samples from normal (non-tumor bearing) dogs and dogs with intra-nasal tumors were collected following routine diagnostic sampling or at the time of necropsy between August 2013 and March 2015. Tissue obtained post-mortem was done so specifically for collection of normal nasal epithelium from dogs that presented for necropsy with no reported clinical signs (e.g. epistaxis, facial swelling or deformity, nasal discharge, or stridor) of an intra-nasal tumor. Routine H&E histopathology was used to confirm normal nasal epithelium from five dogs without nasal tumor and confirm nasal carcinoma in sixteen dogs with nasal tumors. Each tissue sample was divided 3:1 by volume. The larger fraction was placed in formalin and processed for routine H&E staining. The smaller fraction was halved (split 1:1 by volume) and either snap frozen in liquid nitrogen and stored at -80°C or placed in a stabilizing solution to preserve RNA (RNAlater®, Qiagen, Valencia, CA).

### Immunohistochemistry

Samples were reviewed by an anatomical pathologist (JH) and confirmed as normal canine nasal epithelium or nasal carcinomas using routine H&E staining. Immunohistochemical staining was performed for c-KIT (Dako, rabbit polyclonal) at 1:600 dilution<sup>23</sup>, VEGFR2 (Santa Cruz Biotechnology, mouse monoclonal) at 1:75 dilution<sup>24</sup>, PDGFR- $\alpha$  (Santa Cruz Biotechnology, rabbit polyclonal) at 1:500 dilution<sup>25</sup>, PDGFR- $\beta$  (Biogenex, rabbit monoclonal) at 1:100 dilution<sup>23</sup>, and EGFR1 (Invitrogen, mouse monoclonal) at 1:50 dilution<sup>14</sup> on all nasal carcinoma samples. Tissues known to express RTKs of interest [canine mast cell tumor (c-KIT), canine anal sac adenocarcinoma (PDGFR- $\alpha$  & PDGFR- $\beta$ ), canine pyogranulomatous skin (VEGFR2), and normal canine lung (EGFR1)] were used as positive controls for RTK expression.<sup>11,23,24,26,27</sup> Irrelevant isotype matched antibodies at equivalent dilutions were

utilized as negative controls. All slides were immunostained using a Leica Bond Max autostainer. The Bond Polymer Refine Red Detection Kit (Leica Biosystems, Buffalo Grove, IL) which utilizes an alkaline phosphatase-linked polymer with Fast Red chromogen and hematoxylin counterstain was used for four of the antibodies. c-KIT was detected with a similar Bond Polymer Detection Kit that contains a horseradish peroxidase polymer and 3,3-diaminobenzidine (DAB) as the chromogen with a hematoxylin counterstain.

Immunohistochemical staining was quantified on digitized slides utilizing commercial HALO<sup>®</sup> software (Indica Labs, Corrales, NM). Slides were visually evaluated and the region with the highest proportion of immunostained neoplastic cells was annotated to determine the percent of positive staining neoplastic cells. The percent of positive neoplastic cells was identified by using a color deconvolution algorithm in which values are set for stains based on RGB optical densities and intensity channels are established for each stain. The optical density of the entire cell (nucleus, cytoplasm, or membrane) was averaged and if the value was higher than threshold, the cell was considered positive. Tumor stroma staining between non-staining neoplastic cells was also identified.

The percentage of neoplastic cells with positive immunoreactivity were scored according to the following: <5% = 0, 5-25% = 1, 26-50% = 2, and >50% = 3. Cytoplasmic (C), nuclear (N), membranous (M), and stromal (S) staining locations were also identified.

### **RNA isolation and RT-PCR**

Total RNA from normal nasal tissue and carcinomas was obtained using the RNeasy<sup>®</sup> Mini Kit (Qiagen, Valencia, CA) according to manufacturer's instructions from tissue preserved in RNAlater<sup>®</sup> (Qiagen, Valencia, CA). RNA quantity was assessed with a Nanodrop-1000 spectrophotometer (Thermo Scientific, Wilmington, DE). Reverse transcription was carried out

with M-MLV Reverse Transcriptase (Invitrogen™, Carlsbad, CA) using TGradient Thermocycler® (Biometra, Göttingen, Germany) with cycling parameters set at 25°C for 10 minutes, 37°C for 50 minutes, and finally 70°C for 15 minutes. PCR was carried out using cDNA with primers for the genes of interest (Table 2.1), HotStarTaq® Master Mix Kit (Qiagen, Valencia, CA) and TGradient Thermocycler® (Biometra, Göttingen, Germany). Thermal cycling parameters were 95°C for 15 minutes for initial heat activation, followed by 34 cycles of amplifications at 94°C for denaturation for 30 seconds, annealing for 30 seconds, and 72°C for one minute for extension. Samples were then set at 72°C for 10 minutes as the final extension step. The annealing temperature used varied depending on the manufacturer's specifications for that primer (Integrated DNA Technologies, Coralville, IA). Following completion of the PCR reaction, products were separated using 1% agarose gel electrophoresis to resolve and identify PCR products of the expected size. Appropriately sized products were purified with QIAquick® PCR Purification Kit (Qiagen, Valencia, CA) prior to DNA sequencing. Products from the RT-PCR were sequenced using specific primers at the KSU DNA Sequencing and Genotyping Facility (Applied Biosystems 3730 DNA Analyzer) to confirm the identity of the target cDNA. Sequence alignments between canine RT-PCR products and known mammalian RTK sequences were constructed using BLAST® (National Center for Biotechnology Information, U.S National Library of Medicine).

### **Cell lysate preparation and phosphoprotein arrays**

The Proteome Profiler™ Human Phospho-RTK Array Kit (R&D Systems, Minneapolis, MN) was utilized to evaluate *in situ* phosphorylation of 49 different RTKs in nasal carcinoma and normal nasal epithelium samples, an assay previously utilized in canine studies.<sup>11,28</sup> To prepare lysates, 50 mg milligrams of frozen tissue (normal nasal epithelium or nasal carcinoma)

was ground with a liquid nitrogen-cooled mortar and pestle. The powdered tissue was resuspended in a lysis buffer (Lysis Buffer 17, R&D Systems, Minneapolis, MN) supplemented with 10ug/ml pepstatin, 10ug/ml leupeptin, and 10ug/ml aprotinin. The samples were rocked at 4°C for 30 minutes followed by centrifugation at 14,000 x g for 5 minutes. After completion, the supernatant was collected and the protein concentration was quantitated by the Bradford method (Bio-Rad, Hercules, CA). The phosphoprotein arrays were performed according to manufacturer's instructions using 300µg of protein lysate.

Phosphoproteins in nasal tissue samples were detected using a series of 49 specific capture antibodies that were pre-spotted in duplicate on nitrocellulose membranes by the kit manufacturer (R&D Systems, Minneapolis, MN). Each membrane also contained a phosphorylated protein positive control and phosphate buffered saline (PBS) negative control. Membranes were placed in individual trays and incubated for one hour at room temperature with a blocking buffer (Array Buffer 1, R&D Systems, Minneapolis, MN). After removal of the blocking buffer, each membrane was incubated overnight at 4°C with the individual sample protein lysate to allow proteins to bind to fixed antibodies. After binding of phosphorylated and unphosphorylated RTKs, unbound material was removed with Wash Buffer (R&D Systems, Minneapolis, MN) by placing the membranes in individual trays and rocking them for 10 minutes and repeating this washing step a total of three times. Next, the membranes were incubated for two hours at room temperature with an anti-phospho-tyrosine antibody conjugated to horseradish peroxidase (R&D Systems, Minneapolis, MN). Finally, a Chemi Reagent Mix (R&D Systems, Minneapolis, MN) was used to coat the membranes which were subsequently evaluated for chemiluminescence with the FluorChem™ E system (Protein Simple, San Jose, CA).

A subjective positive result was determined by comparing the chemiluminescent result with the positive and negative controls. Positive results were confirmed by averaging pixel density of the pair of duplicate spots representing each RTK using Alphaview Software™ (Protein Simple, San Jose, CA). The intensity of the positive result was recorded by subtracting a background value from the averaged RTK signal. The background value was obtained by averaging the signal from the two PBS negative control spots.

**Table 2.1 Primer Sequences used in RT-PCR**

<b>RTK</b>	<b>Primers</b>	<b>Product Size (bp)</b>
<b>EGFR1</b>	F: 5'- TGG TCC TGG GGA ATT TGG AA- 3' R: 5'- GGT TAT TGC TGA AGC GCA CA- 3'	262
<b>c-KIT</b>	F: 5'- GAG AAC ACA CAC AAC GAA TG- 3' R: 5'- GCA GCG GAC CAG CGT ATC ATT G- 3'	185
<b>PDGFR<math>\alpha</math></b>	F: 5'- GCT CTC ATG TCG GAA CTG AAG- 3' R: 5'- GTG TGC TGT CAT CAG CAG G- 3'	237
<b>PDGFR<math>\beta</math></b>	F: 5'- GAC CAG TCA GTG GAT TAC GTG- 3' R: 5'- GTC TCT CAT GAT GTC ACG AGC CAG- 3'	329
<b>VEGFR2</b>	F: 5'- GTA AGT ACC CTT GTT ATC CAA GCA GCC-3' R: 5' – CGT AGT TCT GTC TGC AGT GCA CCA C- 3'	195

Canine primer sequences with corresponding base pair (bp) product size used in reverse transcriptase polymerase chain reaction (RT-PCR) to assess for qualitative expression. (Urie, BMC Vet Res 2012 and Mariotti, BMC Vet Res 2014)

## **Chapter 3 - Results**

### **Sample Demographics**

Nasal tumor samples (n=16) were collected from untreated tumor-bearing dogs that presented to the Kansas State University Veterinary Health Center (KSU-VHC) between August 2013 and March 2015. The mean age was 11.4 years (median 11.4, range 7.5 to 14.7 years). The majority of the dogs were spayed females (n=8), with the remainder comprising castrated males (n=6) and intact males (n=2). Labrador Retrievers (n=3) and mixed breed dogs (n=3) were represented most often with the remaining population comprised of a single dog representing the following breeds: German wire hair pointer, Shar pei, Australian shepherd, Boxer, American bulldog, Cardigan Welsh corgi, Border collie, Pembroke Welsh corgi, Shetland sheepdog, and Brittany spaniel. All sixteen tumors were histologically classified according to the World Health Organization's histological classification of tumors of the respiratory system of domestic animals.<sup>29</sup> Adenocarcinoma encompassed 50% (n=8) of the tumors while transitional (n=4) and undifferentiated (n=4) nasal carcinomas each comprised 25% of the samples.

### **Immunohistochemistry**

Sixteen nasal carcinoma tissue samples were evaluated for expression of RTKs of interest (Table 3.1 and Figure 3.1). Immunoreactivity for c-KIT was detected in 4/16 samples. Positive immunoreactivity for PDGFR- $\alpha$  was noted in 15/16 samples assessed. Neoplastic cells showed positive immunoreactivity for PDGFR- $\beta$  in only 3/16 samples but strong stromal staining was noted in all 16 samples. EGFR1 immunoreactivity was noted in 14/16 samples. All samples showed immunoreactivity for VEGFR2. Normal nasal epithelium demonstrated variable positive immunoreactivity for VEGFR2 (4/5 positive), PDGFR- $\alpha$  (3/5 positive), PDGFR- $\beta$  (2/5 positive) and EGFR1 (3/5 positive). No reactivity was expressed for c-KIT.



## Reverse Transcriptase-Polymerase Chain Reaction (RT-PCR)

Successful extraction of mRNA was obtained from all normal nasal and nasal carcinoma samples (Table 3.2). Messenger RNA for c-KIT, PDGFR- $\beta$ , and VEGFR2 was present in all sixteen tumors assessed; however, messenger RNA for PDGFR- $\alpha$  and EGFR1 was detected in only 15/16 (93.7%) samples. Messenger RNA for all RTKs were detected in normal nasal tissue.

## Phosphoprotein Arrays

The phosphorylation status of forty-nine RTKs was assessed in sixteen nasal carcinoma and five normal nasal samples [Table 3.3 and Figure 3.2]. Specific RTKs that were phosphorylated in >50% of tumors were Insulin-R (68.7%), EGFR1 (62.5%) and ROR2 (56.2%). Phosphorylated RTKs in 25-50% of tumors were ALK (43.7%), RYK (37.5%), DTK (31.3%), and Tie-1 (25%). Five normal nasal epithelium samples showed phosphorylation of Insulin R in 80% of samples, whereas phosphorylation of EGFR1, RYK, and ROR2 was identified in 60% of samples assessed. None of the nasal carcinoma or normal nasal epithelium samples had phosphorylation of VEGFR2, PDGFR- $\alpha$ , PDGFR- $\beta$ , or c-KIT.

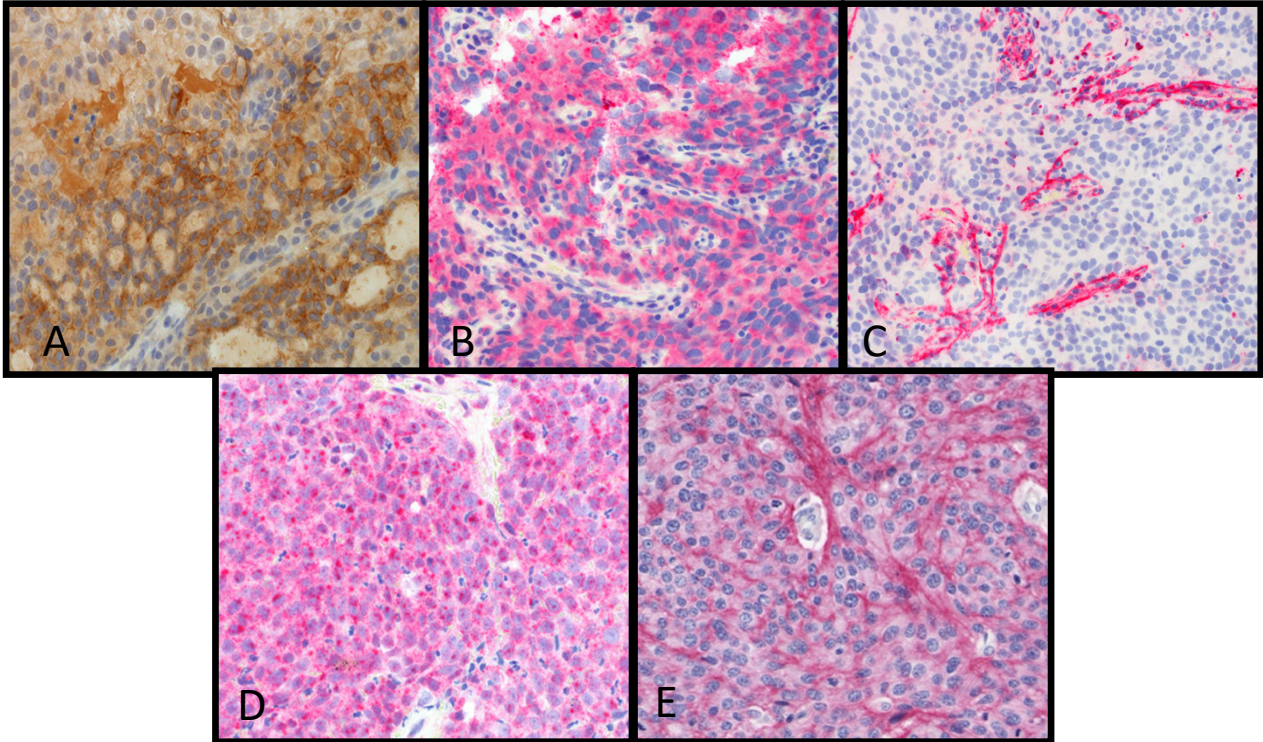
**Table 3.1 Nasal carcinoma RTK expression by IHC**

RTK	0 n (%)	1 n (%)	2 n (%)	3 n (%)	Predominant Localization
<b>c-KIT</b>	12 (75.0)	3 (18.7)	1 (6.3)	0	C
<b>VEGFR2</b>	0	0	1 (6.3)	15 (93.7)	C
<b>PDGFR<math>\alpha</math></b>	1 (6.3)	0	2 (12.5)	13 (81.2)	N, C
<b>PDGFR<math>\beta</math></b>	13 (81.2)	0	1 (6.3)	2 (12.5)	S
<b>EGFR1</b>	2 (12.5)	2 (12.5)	5 (31.3)	7 (43.7)	M

N: nuclear; M: membranous; C: cytoplasmic; S: tumor stroma

The number (n) of positive canine nasal carcinoma samples evaluated by immunohistochemistry (IHC). The percentage of neoplastic cells with positive immunoreactivity were scored according to the following: <5% = 0, 5-25% = 1, 26-50% = 2, and >50% = 3.

**Figure 3.1 Immunohistochemistry for KIT, VEGFR2, PDGFR- $\beta$ , PDGFR- $\alpha$  & EGFR**



Representative images of each receptor tyrosine kinase (RTK) examined are shown. (Panel A: c-KIT cytoplasmic staining, Panel B: VEGFR2 cytoplasmic staining, Panel C: PDGFR $\beta$  stromal staining, Panel D: PDGFR $\alpha$  nuclear and cytoplasmic staining, Panel E: EGFR1 membranous staining). 400X.

**Table 3.2 Nasal carcinoma qualitative messenger RNA expression by RT-PCR**

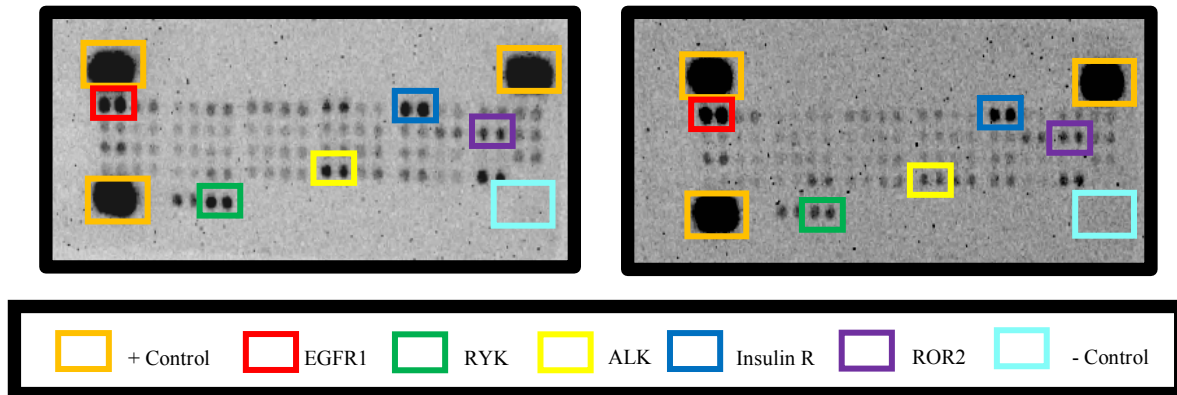
Sample #	VEGFR2	PDGFR- $\alpha$	PDGFR- $\beta$	KIT	EGFR1
1	+	+	+	+	+
2	+	+	+	+	+
3	+	+	+	+	+
4	+	+	+	+	+
5	+	+	+	+	+
6	+	-	+	+	+
7	+	+	+	+	+
8	+	+	+	+	-
9	+	+	+	+	+
10	+	+	+	+	+
11	+	+	+	+	+
12	+	+	+	+	+
13	+	+	+	+	+
14	+	+	+	+	+
15	+	+	+	+	+
16	+	+	+	+	+

**Table 3.3 Nasal carcinoma phosphoprotein results**

RTK	n (%)
Insulin R	11 (68.7)
EGFR1	10 (62.5)
ROR2	9 (56.2)
ALK	7 (43.7)
RYK	6 (37.5)
DTK	5 (31.3)
Tie-1	4 (25%)

The number (n) of the most common phosphorylated receptor tyrosine kinases (RTK) from sixteen canine nasal carcinoma samples evaluated by The Proteome Profiler™ Human Phospho-RTK Array Kit.

**Figure 3.2 Phospho-RTK arrays of canine nasal carcinomas**



On the representative example arrays shown from two tumors, positive and negative controls, insulin receptor (Insulin R), epidermal growth factor receptor 1 (EGFR1), receptor tyrosine kinase-like orphan receptor 2 (ROR2), anaplastic lymphoma kinase (ALK), and receptor-like tyrosine kinase (RYK) have been identified.

## Chapter 4 – Discussion

The results of this study suggest that canine nasal carcinomas do not demonstrate persistent phosphorylation of VEGFR2, PDGFR- $\alpha$ , PDGFR- $\beta$ , and c-KIT. Thus, inhibition of these RTKs is not the principle mechanism by which toceranib exerts its clinical effects on this tumor type. Although phosphorylation of these RTKs was not detected, the presence of each RTK demonstrated by detection of messenger RNA and immunoreactive protein, in nasal carcinoma and normal nasal epithelium was verified. Thus, although the key angiogenic targets for toceranib action are present, the absence of phosphorylation of these RTKs suggests the conclusion that any clinical effect of toceranib may occur through inhibition of alternative unidentified RTK pathway in canine nasal carcinomas. Additionally, normal canine nasal epithelium expressed a similar spectrum of RTKs to those identified in the neoplastic tissue, further supporting the idea of an unidentified RTK pathway as a possible underlying means of toceranib's clinical efficacy. However, the lack of phosphorylation in the nasal carcinoma tissue does not completely eliminate the possibility that these RTKs have a role in this tumor's biology or contribute in an indirect anti-tumor action of toceranib.

Multiple RTK targets of toceranib, particularly PDGFR- $\beta$ , play crucial roles in the tumor microenvironment (TME) and their presence is documented by strong stromal expression.<sup>30,31</sup> Stromal expression of PDGFR- $\beta$  was present in all samples analyzed in this study whereas previous studies have shown only 60.9% of samples to have stromal staining for PDGFR- $\beta$ .<sup>13</sup> The development and function of vessels in the TME rely heavily on PDGFR- $\beta$  and inhibition of this RTK in the TME has been documented in some human solid tumors and may represent an indirect target for toceranib in canine nasal carcinomas.<sup>30,32,33</sup> Interestingly, VEGFR2 and PDGFR- $\alpha$  were not expressed in the tumor stroma in this study; however, PDGFR- $\alpha$  was shown

to have nuclear localization. Nuclear localized RTKs have been shown to bypass standard signal transduction and respond to stimuli through transcriptional and translational regulation of target genes.<sup>34</sup> Nuclear localized RTKs, such as PDGFR- $\alpha$ , have been observed in highly proliferative normal tissues and neoplastic tissues that have an elevated signaling for cell growth, survival and differentiation.<sup>34-38</sup> The identified nuclear localization of PDGFR- $\alpha$  in nasal carcinoma tissues in this study may suggest that it has important implication in the development of this cancer; however, further investigation into its role is warranted.

Aberrant function of EGFR1 has been implicated as an important oncogenic driver in a number of human cancers and the results of this study suggest that EGFR1's noted phosphorylation in over half of the nasal carcinoma samples may represent a possible role in tumorigenesis.<sup>20,39-41</sup> Nearly all the samples analyzed in this study showed EGFR1's presence at the protein and messenger RNA level in comparison to a previously noted 55% of canine nasal carcinomas and 74% of human nasopharyngeal carcinomas.<sup>14,42</sup> The discrepancy between the number of samples exhibiting phosphorylation and protein/messenger RNA expression in this study may tell us that while EGFR1 is expressed in most canine nasal carcinomas, only a subset may be in a persistently phosphorylated state. In addition to EGFR1 phosphorylation by nasal carcinomas, normal nasal epithelium evaluated within this study was shown to have high EGFR1 phosphorylation. With the concurrent phosphorylation of normal nasal epithelium and nasal carcinoma tissue, further investigation into possible activating mutations or autocrine paracrine loops as a cause of persistent phosphorylation within the nasal carcinoma tissue is warranted to further elucidate EGFR1's role in nasal carcinoma tumorigenesis, as well as its role as a future therapeutic target.<sup>43,44</sup>

Phosphorylation of several RTK pathways were identified in the nasal carcinoma samples in this study including those involved in key Hallmarks of Cancer such as angiogenesis, metastasis, tissue invasion, and limitless replicative potential.<sup>45</sup> For example, tyrosine kinase with immunoglobulin-like and EGF like domains 1 (Tie-1) and anaplastic lymphoma kinase (ALK) were phosphorylated in nasal carcinoma tissue in this study and have both been associated with neoplastic angiogenesis and metastasis of neoplastic cells.<sup>46-50</sup> Additionally, receptor tyrosine kinase-like orphan receptor 2 (ROR2), tyrosine-protein kinase DTK (DTK), and receptor-like tyrosine kinase (RYK), all exhibiting phosphorylation in this study, have been noted to participate in neoplastic tissue invasion and cellular proliferation.<sup>51-56</sup> The phosphorylation of these RTKs in canine nasal carcinoma indicates that they may participate in the development, progression, and eventual metastasis of this tumor type; however, further investigation into their specific roles in canine nasal carcinomas is needed. Furthermore, the phosphorylation of these RTKs in canine nasal carcinoma samples may represent additional novel therapeutic targets.

This study's descriptive design imparts various limitations including small study size, tumor heterogeneity, and tumor sample size. The small study size represents only a limited spectrum of the population of dogs afflicted by nasal carcinomas and evaluating a larger number of nasal carcinoma samples would allow for applicability of these results with more certainty. As with many tumors, nasal carcinomas are heterogeneous in their composition and the tumor sample sizes in this study were small due to collection methodology. The combination of tumor heterogeneity and small sample size presents the possibility of misrepresenting true RTK phosphorylation and expression in the samples analyzed due to heterogeneous RTK distribution.

## **Chapter 5 – Conclusions**

Major RTK targets of toceranib were not phosphorylated in the canine nasal carcinomas evaluated. However, the presence of the RTKs inhibited by toceranib were verified by positive protein and messenger RNA expression. The lack of phosphorylated target RTKs in canine nasal carcinomas suggests that toceranib may be exerting its clinical effects through an unidentified mechanism. Furthermore, stromal expression of PDGFR- $\beta$  in the tumor microenvironment may provide an indirect method by which toceranib functions in this tumor type. The results also demonstrated that several key RTKs, including EGFR1, were phosphorylated in the majority of samples analyzed. The phosphorylation of EGFR1 and other RTKs warrants further investigation into their role in this tumor type and consideration as novel targets for the treatment of canine nasal carcinoma.



## References

1. Madewell BR, Priester WA, Gillette EL, et al. Neoplasms of the nasal passages and paranasal sinuses in domesticated animals as reported by 13 veterinary colleges. *Am J Vet Res* 1976;37:851–856.
2. Lana SE, Dernell WS, Lafferty MH, et al. Use of radiation and a slow-release cisplatin formulation for treatment of canine nasal tumors. *Vet Radiol Ultrasound* 2004;45:577–581.
3. Patnaik AK. Canine sinonasal neoplasms: clinicopathological study of 285 cases. *J Am Anim Hosp Assoc* 1989;25:103-114
4. Adams WM, Kleiter MM, Thrall DE, et al. Prognostic significance of tumor histology and computed tomographic staging for radiation treatment response of canine nasal tumors. *Vet Radiol Ultrasound* 2009;50:330–335.
5. Kubicek L, Milner R, An Q, et al. Outcomes and Prognostic Factors Associated with Canine Sinonasal Tumors Treated with Curative Intent Cone-Based Stereotactic Radiosurgery (1999-2013). *Vet Radiol Ultrasound* 2016;57:331–340.
6. Lawrence JA, Forrest LJ, Turek MM, et al. Proof of principle of ocular sparing in dogs with sinonasal tumors treated with intensity-modulated radiation therapy. *Vet Radiol Ultrasound* 2010;51:561–570.
7. Rassnick KM, Goldkamp CE, Erb HN, et al. Evaluation of factors associated with survival in dogs with untreated nasal carcinomas: 139 cases (1993-2003). *J Am Vet Med Assoc* 2006;229:401–406.
8. Downing S, Chien MB, Kass PH, et al. Prevalence and importance of internal tandem duplications in exons 11 and 12 of c-kit in mast cell tumors of dogs. *Am J Vet Res* 2002;63:1718–1723.
9. London CA, Hannah AL, Zadovoskaya R, et al. Phase I dose-escalating study of SU11654, a small molecule receptor tyrosine kinase inhibitor, in dogs with spontaneous malignancies. *Clin Cancer Res* 2003;9:2755–2768.
10. London C, Mathie T, Stingle N, et al. Preliminary evidence for biologic activity of toceranib phosphate (Palladia®) in solid tumours. *Vet Comp Oncol* 2012;10:194–205.
11. Urie BK, Russell DS, Kisseberth WC, et al. Evaluation of expression and function of vascular endothelial growth factor receptor 2, platelet derived growth factor receptors-alpha and -beta, KIT, and RET in canine apocrine gland anal sac adenocarcinoma and thyroid carcinoma. *BMC Vet Res* 2012;8:67.
12. Mendel DB, Laird AD, Xin X, et al. In vivo antitumor activity of SU11248, a novel tyrosine kinase inhibitor targeting vascular endothelial growth factor and platelet-derived growth factor

receptors: determination of a pharmacokinetic/pharmacodynamic relationship. *Clin Cancer Res* 2003;9:327–337.

13. Gramer I, Killick D, Scase T, et al. Expression of VEGFR and PDGFR- $\alpha$ / $\beta$  in 187 canine nasal carcinomas. *Vet Comp Oncol* 2017;15:1041–1050.
14. Shiomitsu K, Johnson CL, Malarkey DE, et al. Expression of epidermal growth factor receptor and vascular endothelial growth factor in malignant canine epithelial nasal tumours. *Vet Comp Oncol* 2009;7:106–114.
15. Bernabe LF, Portela R, Nguyen S, et al. Evaluation of the adverse event profile and pharmacodynamics of toceranib phosphate administered to dogs with solid tumors at doses below the maximum tolerated dose. *BMC Vet Res* 2013;9:190.
16. Hanazono K, Fukumoto S, Kawamura Y, et al. Epidermal growth factor receptor expression in canine transitional cell carcinoma. *J Vet Med Sci* 2015;77:1–6.
17. Fraser AR, Bacci B, le Chevoir MA, et al. Epidermal Growth Factor Receptor and Ki-67 Expression in Canine Gliomas. *Vet Pathol* 2016;53:1131–1137.
18. Araújo MR, Campos LC, Damasceno KA, et al. HER-2, EGFR, Cox-2 and Ki67 expression in lymph node metastasis of canine mammary carcinomas: Association with clinical-pathological parameters and overall survival. *Res Vet Sci* 2016;106:121–130.
19. Mariotti ET, Premanandan C, Lorch G. Canine pulmonary adenocarcinoma tyrosine kinase receptor expression and phosphorylation. *BMC Vet Res* 2014;10:19.
20. Grandis JR, Tweardy DJ. Elevated levels of transforming growth factor alpha and epidermal growth factor receptor messenger RNA are early markers of carcinogenesis in head and neck cancer. *Cancer Res* 1993;53:3579–3584.
21. Zimmermann M, Zouhair A, Azria D, et al. The epidermal growth factor receptor (EGFR) in head and neck cancer: its role and treatment implications. *Radiat Oncol* 2006;1:11.
22. London CA. Kinase dysfunction and kinase inhibitors. *Vet Dermatol* 2013;24:181–187.
23. Brown RJ, Newman SJ, Durtschi DC, et al. Expression of PDGFR- $\beta$  and Kit in canine anal sac apocrine gland adenocarcinoma using tissue immunohistochemistry. *Vet Comp Oncol* 2012;10:74–79.
24. Yonemaru K, Sakai H, Murakami M, et al. Expression of vascular endothelial growth factor, basic fibroblast growth factor, and their receptors (flt-1, flk-1, and flg-1) in canine vascular tumors. *Vet Pathol* 2006;43:971–980.
25. Higgins RJ, Dickinson PJ, LeCouteur RA, et al. Spontaneous canine gliomas: overexpression of EGFR, PDGFR $\alpha$  and IGF2 demonstrated by tissue microarray immunophenotyping. *J Neurooncol* 2010;98:49–55.

26. Sabattini S, Mancini FR, Marconato L, et al. EGFR overexpression in canine primary lung cancer: pathogenetic implications and impact on survival. *Vet Comp Oncol* 2014;12:237–248.
27. Thompson JJ, Yager JA, Best SJ, et al. Canine subcutaneous mast cell tumors: cellular proliferation and KIT expression as prognostic indices. *Vet Pathol* 2011;48:169–181.
28. McCleese JK, Bear MD, Kulp SK, et al. Met interacts with EGFR and Ron in canine osteosarcoma. *Vet Comp Oncol* 2013;11:124–139.
29. Dungworth DL, Pathology ARO, WHO Collaborating Center for Worldwide Reference on Comparative Oncology. *Histological Classification of Tumors of the Respiratory System of Domestic Animals*. Armed Forces Institute of Pathology; 1999.
30. Ostman A. PDGF receptors-mediators of autocrine tumor growth and regulators of tumor vasculature and stroma. *Cytokine Growth Factor Rev* 2004;15:275–286.
31. Pietras K, Pahler J, Bergers G, et al. Functions of paracrine PDGF signaling in the proangiogenic tumor stroma revealed by pharmacological targeting. Sawyers CL, ed. *PLoS Med* 2008;5:e19.
32. Ferrara N, Kerbel RS. Angiogenesis as a therapeutic target. *Nature* 2005;438:967–974.
33. Lewis NL, Lewis LD, Eder JP, et al. Phase I Study of the Safety, Tolerability, and Pharmacokinetics of Oral CP-868,596, a Highly Specific Platelet-Derived Growth Factor Receptor Tyrosine Kinase Inhibitor in Patients With Advanced Cancers. *Journal of Clinical Oncology* 2016;27:5262–5269.
34. Du Y, Hsu JL, Wang Y-N, et al. Nuclear Functions of Receptor Tyrosine Kinases. In: *Receptor Tyrosine Kinases: Structure, Functions and Role in Human Disease*. 1st ed. Nuclear Functions of Receptor Tyrosine Kinases. New York, NY: Springer New York; 2014:77–109.
35. Aslam MI, Hettmer S, Abraham J, et al. Dynamic and nuclear expression of PDGFR $\alpha$  and IGF-1R in alveolar Rhabdomyosarcoma. *Mol Cancer Res* 2013;11:1303–1313.
36. Lin SY, Makino K, Xia W, et al. Nuclear localization of EGF receptor and its potential new role as a transcription factor. *Nat Cell Biol* 2001;3:802–808.
37. Marti U, Burwen SJ, Wells A, et al. Localization of epidermal growth factor receptor in hepatocyte nuclei. *Hepatology* 1991;13:15–20.
38. Stachowiak MK, Fang X, Myers JM, et al. Integrative nuclear FGFR1 signaling (INFS) as a part of a universal “feed-forward-and-gate” signaling module that controls cell growth and differentiation. *J Cell Biochem* 2003;90:662–691.
39. Arteaga CL. ErbB-targeted therapeutic approaches in human cancer. *Exp Cell Res* 2003;284:122–130.

40. Dei Tos AP, Ellis I. Assessing epidermal growth factor receptor expression in tumours: what is the value of current test methods? *Eur J Cancer* 2005;41:1383–1392.
41. Gan HK, Kaye AH, Luwor RB. The EGFRvIII variant in glioblastoma multiforme. *J Clin Neurosci* 2009;16:748–754.
42. Pan J, Kong L, Lin S, et al. The clinical significance of coexpression of cyclooxygenases-2, vascular endothelial growth factors, and epidermal growth factor receptor in nasopharyngeal carcinoma. *Laryngoscope* 2008;118:1970–1975.
43. Mantovani FB, Morrison JA, Mutsaers AJ. Effects of epidermal growth factor receptor kinase inhibition on radiation response in canine osteosarcoma cells. *BMC Vet Res* 2016;12:82.
44. Paul MK, Mukhopadhyay AK. Tyrosine kinase - Role and significance in Cancer. *Int J Med Sci* 2004;1:101–115.
45. Hanahan D, Weinberg RA. Hallmarks of cancer: the next generation. *Cell* 2011;144:646–674.
46. Capelletti M, Gelsomino F, Tiseo M. MET and ALK as targets for the treatment of NSCLC. *Curr Pharm Des* 2014;20:3914–3932.
47. Seegar TCM, Eller B, Tzvetkova-Robev D, et al. Tie1-Tie2 interactions mediate functional differences between angiopoietin ligands. *Mol Cell* 2010;37:643–655.
48. Singh H, Tahir TA, Alawo DOA, et al. Molecular control of angiopoietin signalling. *Biochem Soc Trans* 2011;39:1592–1596.
49. Wallace GC, Dixon-Mah YN, Vandergrift WA, et al. Targeting oncogenic ALK and MET: a promising therapeutic strategy for glioblastoma. *Metab Brain Dis* 2013;28:355–366.
50. Yang P, Chen N, Jia J-H, et al. Tie-1: A potential target for anti-angiogenesis therapy. *J Huazhong Univ Sci Technol Med Sci* 2015;35:615–622.
51. Debebe Z, Rathmell WK. Ror2 as a therapeutic target in cancer. *Pharmacol Ther* 2015;150:143–148.
52. Duan Y, Wong W, Chua SC, et al. Overexpression of Tyro3 and its implications on hepatocellular carcinoma progression. *Int J Oncol* 2016;48:358–366.
53. Ekyalongo RC, Mukohara T, Funakoshi Y, et al. TYRO3 as a potential therapeutic target in breast cancer. *Anticancer Res* 2014;34:3337–3345.
54. Green J, Nusse R, van Amerongen R. The role of Ryk and Ror receptor tyrosine kinases in Wnt signal transduction. *Cold Spring Harb Perspect Biol* 2014;6:a009175–a009175.
55. Rasmussen NR, Debebe Z, Wright TM, et al. Expression of Ror2 mediates invasive phenotypes in renal cell carcinoma. Nie D, ed. *PLoS ONE* 2014;9:e116101.

56. Schmitz R, Valls AF, Yerbes R, et al. TAM receptors Tyro3 and Mer as novel targets in colorectal cancer. *Oncotarget* 2016;7:56355–56370.

## Appendix A – Abbreviations

ALK	anaplastic lymphoma kinase
bp	base pair
°C	Celsius
cDNA	complementary deoxyribonucleic acid
c-KIT	stem cell factor receptor
CSFR1	colony stimulating factor receptor 1
DAB	3,3-diaminobenzidine
DNA	deoxyribonucleic acid
DTK	tyrosine-protein kinase DTK
EGFR1	epidermal growth factor receptor 1
F	forward
FDA	Food and Drug Administration
FLT-3	FMS-like tyrosine kinase 3
H & E	hematoxylin and eosin
IHC	immunohistochemistry
Insulin-R	insulin receptor
KSU	Kansas State University
µg	microgram
mRNA	messenger ribonucleic acid
PBS	phosphate buffered saline
PCR	polymerase chain reaction
PDGFR-α	platelet derived growth factor alpha
PDGFR-β	platelet derived growth factor receptor beta
R	reverse
RGB	red-green-blue
RNA	ribonucleic acid
ROR2	receptor tyrosine kinase-like orphan receptor 2
RTK	receptor tyrosine kinase
RT-PCR	reverse transcriptase polymerase chain reaction
RYK	receptor-like tyrosine kinase

Tie-1	tyrosine kinase with immunoglobulin-like and EGF like domains 1
TME	tumor microenvironment
VEGF	vascular endothelial growth factor
VEGFR2	vascular endothelial growth factor receptor-2
VHC	Veterinary Health Center

**Appendix B – Complete Phospho-RTK Results  
(Number of samples phosphorylated)**

EGFR	10
ErbB2	1
ErbB3	1
ErbB4	2
FGF R1	3
FGF R2-alpha	3
FGF R3	2
FGF R4	1
Insulin R	11
IGF-1 R	1
Axl	2
Dtk	5
Mer	2
HGF R	1
MSP R	1
PDGFR-alpha	0
PDGFR-beta	0
KIT	0
Flt-3	0



M-CSF R	1
c-RET	2
ROR1	2
ROR2	9
Tie-1	4
Tie-2	3
TrkA	1
TrkB	1
TrkC	1
VEGFR1	0
VEGFR2	0
VEGFR3	0
MuSK	1
EphA1	1
EphA2	1
EphA3	0
EphA4	2
EphA6	2
EphA7	1
EphB1	1
EphB2	3

EphB4	1
EphB6	2
ALK	7
DDR1	3
DDR2	4
EphA5	1
EphA10	4
EphB3	4
RYK	6